Biochimica et Biophysica Acta 1848 (2015) 3197–3204

Contents lists available at ScienceDirect

Biochimica et Biophysica Acta

journal homepage: www.elsevier.com/locate/bbamem

Tectonics of a K^+ channel: The importance of the N-terminus for channel gating

F. Hoffgaard [a,b], S.M. Kast [b], A. Moroni [c], G. Thiel [d], K. Hamacher [a]

[a] Computational Biology & Simulation Group, Dept. of Biology, TU Darmstadt, Germany
[b] Physikalische Chemie III, TU Dortmund, Germany
[c] Dipartimento di Biologia, Università degli Studi di Milano e Istituto di Biofisica, CNR, Milano, Italy
[d] Membrane Biophysics Group, Dept. of Biology, TU Darmstadt, Germany

ARTICLE INFO

Article history:
Received 5 August 2015
Received in revised form 9 September 2015
Accepted 18 September 2015
Available online 25 September 2015

Keywords:
Ion channels
Computational biophysics
Structure-function correlates
Reduced molecular models
Kcv

ABSTRACT

The small K^+ channel Kcv represents the pore module of complex potassium channels. It was found that its gating can be modified by sensor domains, which are N-terminally coupled to the pore. This implies that the short N-terminus of the channel can transmit conformational changes from upstream sensors to the channel gates. To understand the functional role of the N-terminus in the context of the entire channel protein, we apply combinatorial screening of the mechanical coupling and long-range interactions in the Kcv potassium channel by reduced molecular models. The dynamics and mechanical connections in the channel complex show that the N-terminus is indeed mechanically connected to the pore domain. This includes a long rang coupling to the pore and the inner and outer transmembrane domains. Since the latter domains host the two gates of the channel, the data support the hypothesis that mechanical perturbation of the N-terminus can be transmitted to the channel gates. This effect is solely determined by the topology of the channel; sequence details only have an implicit effect on the coarse-grained dynamics via the fold and not through biochemical details at a smaller scale. This observation has important implications for engineering of synthetic channels on the basis of a K^+ channel pore.

1. Introduction

Potassium channels are responsible for the passive and highly selective flux of K^+ ions down a concentration gradient. Common to all K^+-channels is the central pore module [1]. It comprises two transmembrane (TMD) helices separated by the pore helix [2]. Four units assemble such that the pore loops come together to form a selectivity filter for the ions to pass. Although all K^+ − channel proteins have maintained this overall topology of the pore module throughout evolution, only the K^+ signature sequence alone is highly conserved on an amino acid (AA) basis. With only minor deviations, this domain is in all K^+ channels composed of the motifs TxxTxGYG or TxxTxGFG [3]. In the tetrameric pore module this sequence forms the selectivity filter [4].

While the selectivity filter and the gates, which control the activity of the channel, are well understood individually, it remains unclear to this day how different domains in a channel are functionally communicating with each other via long-range interactions. For instance some channels are regulated by ligands such as ATP in K_{ATP}-channels or cAMP in CNG channels, which bind to cytosolic domains of the protein [5–7]. This binding is then transferred via unknown mechanical interactions to the gates in the pore module. Such mechanical connections are also relevant for the gating of voltage-dependent K^+ (K_V) channels, which depend on a movement of the voltage sensor. This domain is adjacent to the pore module and undergoes a dislocation in response to a voltage across the membrane. This movement of the voltage sensor domain (VSD) [8] must then be translated by mechanical interaction into conformational changes in the pore module to operate the gates [8,9].

In the present study, we use a biophysical and structural approach to uncover such long-range interactions in one of the simplest K^+ channel, the miniature channel Kcv. This 94 amino acid protein is among the smallest proteins known to form a functional K^+-channel; from a structural point of view it basically corresponds to the aforementioned "pore module" of all known K^+-channels [10]. In spite of its small size the Kcv channel already exhibits many of the features of complex K^+-channels [10]. This includes ion selectivity, gating and sensitivity to channel blockers [11,12]. An analysis of structure/function correlates has discovered two distinct gates in this channel. One gate, which is responsible for a fast gating at extreme negative and positive voltages, can be attributed to a depletion of ions in the selectivity filter [13]. A second gate, which is presumably responsible for a slow activation of the channel at negative voltages, was attributed to salt bridges at the cytosolic entry into the channel. The salt bridge partners for this gate are provided by charges in the N-terminal slide helix of the channel and the charged carboxyl terminus of the inner transmembrane domain [14,15].

http://dx.doi.org/10.1016/j.bbamem.2015.09.015
0005-2736/

The starting point of the present study is the finding that the gating of the channel can be modified by a naïve coupling of the Kcv channel at the N-terminus with regulatory domains [16–18]. The N-terminal coupling of a voltage sensor from a phosphatase from *Chiona intestinalis* converted the Kcv channel from a voltage independent channel into a slow activating outward rectifier [16]. By an N-terminal connection with a blue light sensor from plants the channel acquired a specific light sensitivity [17]. These data suggest that a small movement of the voltage sensor in the membrane [8], which is evoked by a change in the electrical field, is mechanically transmitted to the channel pore and finally to the gate(s) in the pore. The experimental data show that this coupling between VSD and the pore is depending on the length of the linker domain. This advocates a system according to which the movement of the VSD is mechanically coupled via the linker to the outer transmembrane domain, e.g. the domain to which the linker is coupled. In order to understand how a movement of the N-terminus in Kcv, e.g. the structure, which corresponds to the linker in Kv_{synt}, should be transmit to other parts of the channel and presumably to the gates, we use anisotropic network model [19,20]. By comparing our model predictions with experimental data we uncover long long-range interactions in the pore module, which are able of coupling conformational changes in the N-terminus to distant domains relevant for gating of the channel. As a model system we use a Kcv geometry [21] (structural data are provided as supplementary information [Kcv-HOM-K29deprot_BiophysJ_96_485_2009.pdb], referred to under the acronym Kcv-HOM-$K29_{deprot}$ in Ref. [21]) that has been obtained by symmetrizing results from extensive molecular dynamics simulation [14]. This structure proved already adequate to predict and explain a bulk of structure/function relations in this small channel [15,21–23]. In the present study, we are confronted with a *combinatorially* large number of simulations, while at the same time we are solely interested in the dynamical behavior around the native state of the protein. These two aspects render all-atom molecular dynamics simulations technically not feasible while not contributing any additional insight. We therefore employ coarse-grained molecular models as laid out in the Methods section.

2. Theory/calculation

The underlying principle of elastic network models is to view a folded protein as a mechanical network of amino acids [24,25]. We reduce the complexity of proteins to a graph, whose nodes are the residues of the folded protein, each represented by a bead located at the position of its respective C_α atom. The edges in the network represent physical interactions, which in turn are reduced to harmonic interactions for all nodes (residues) being closer than a certain cutoff distance r_c. As worked out in previous studies, a physically sound choice is $r_c =$ 13 Å as distance cutoff [25–28].

2.1. Anisotropic network models

Anisotropic network models (ANMs) [25] are an extension of so-called Gaussian network models [24]. While the latter model fluctuations of residues in a protein structure isotropically, ANMs invoke anisotropy of the fluctuations in order to assess directionality of correlated motions. All interactions are modeled by Hookean potentials. The individual interaction potential terms are weighted inversely by the distance separating the residues under consideration [27,29]. Instead of the $N \times N$ Kirchhoff matrix of polymer physics, we now deal with the $3N \times 3N$ Hessian matrix that is composed of N^2 super elements H_{ij} of the form

$$\mathbf{H}_{ij} = \begin{bmatrix} \partial^2 V/\partial X_i \partial X_j & \partial^2 V/\partial X_i \partial Y_j & \partial^2 V/\partial X_i \partial Z_j \\ \partial^2 V/\partial Y_i \partial X_j & \partial^2 V/\partial Y_i \partial Y_j & \partial^2 V/\partial Y_i \partial Z_j \\ \partial^2 V/\partial Z_i \partial X_j & \partial^2 V/\partial Z_i \partial Y_j & \partial^2 V/\partial Z_i \partial Z_j \end{bmatrix} \quad (1)$$

where X_i, Y_i, and Z_i are the components of the position vector r_i of individual sites i. The full potential V is given by

$$V = \frac{\alpha}{a^2}\left[\frac{aK}{2}\sum_i \left(s_{i,i+1} - s^0_{i,i+1}\right)^2 + \sum_{(i,j)\in I'} \frac{\kappa_{ij}}{2}\left(s_{ij} - s^0_{ij}\right)^2\right] \quad (2)$$

where s_{ij} are the spatial separations of residues i and j, the superscript indicates the native configuration. K and κ_{ij} weight the interactions of covalent and non-covalent interactions, respectively. I' is defined as the set of all non-covalent interactions between residues i and j closer than r_c, while the first sum is Eq. (2) covers all covalent interactions. The scaling constants a and α were introduced to fit experimental B factors [29]. For the homogeneous parameterization, we use a universal force constant $\kappa = K = \kappa_{ij} = 1$ to describe the interaction of any contacting residue pair (i,j) as put forward by Tirion [30], whereas for the inhomogeneous parameterization we distinguish between bonded and non-bonded contacts and set $\kappa_{ij} = 3.17RT$ and $K = 83.33RT$ as previously established [31]. The pseudo-inverse of the Hessian constitutes the mechanical covariance matrix C and resembles the correlated motions, split into x, y, z directions, of any pair of residues in the thermodynamic ensemble.

This matrix is computed via singular value decomposition (SVD) [32]. Experimental B factors can be reproduced from C [25,29]. Introducing mutations by setting contacts artificially to zero or by changing interaction potentials leads to altered covariance matrices C^{mut}. To quantify the magnitude of change in the protein dynamics introduced by mutations, we use the Frobenius norm

$$d = \sqrt{\sum_{ij}\left(\mathbf{C}_{ij} - \mathbf{C}^{mut}_{ij}\right)^2} \quad (3)$$

Computing the Frobenius norm solely for the whole matrix may disguise relevant changes that occur only in functional subregions. To cope with such obscuration effects, we compute the Frobenius norm for several well defined parts of the protein and, therefore, its covariance matrix as well. We defined structurally and functionally interesting channel regions [14,21].

From the mechanical covariances one can additionally compute the correlation matrices by dividing each matrix entry by the square root of its corresponding diagonal elements. To investigate the correlation of motions, we performed this step and again restricted the subsequent Frobenius norm computations to the functional portions of the channel.

2.2. Parameterization of the anisotropic network models

We used the following two different weighting schemes for the parameterization of the interaction potentials, which describe the harmonic spring connections between each of two residues that are in contact in the native Kcv structure:

(a) *homogeneous* parameterization, that does not discriminate between covalent and non-covalent bonds; this effectively focuses exclusively on structural aspects;
(b) *inhomogeneous* parameterization, ensuring that covalent bonds are more rigid in comparison to non-covalent contacts within the protein structure.

We found that our results do *not* depend on these choices (Fig. S1). We, therefore, show only results for the homogenous case here.

2.3. Switching-off interactions in the channel protein

In this part of the study we mimic the effect of mutations by artificially switching off contacts in an ANM for the Kcv structure giving rise to a mutated mechanical covariance matrix C^{mut}. This is equivalent

to setting the interaction strength locally to a vanishing value. Since the Kcv channel is in its functional state a homotetramer, we simultaneously switch off corresponding contacts in all chains. We consider the following scenarios: Each non-covalent contact within a chain is switched off separately, thus its force constant is set to zero in all chains of the homotetramer at a time. Note that the problem of additional singularities does not occur due to the high connectivity of each residue. Therefore, the preservation of at least two contacts (one covalent, one non-covalent) for each residue is guaranteed.

2.4. In silico experiments on ΔN terminal mutants

Removing corresponding residues in each chain at the N-terminus generates ΔN mutants. We focus on the Δ7, Δ8 and Δ9 mutants, which lack the first 7, 8 and 9 N-terminal amino acids, respectively. We construct an ANM model for each mutant and compute the difference matrix of the covariance matrices of Δ7 and Δ9, which is restricted to entries of residues that are present in both mutants. We then proceed to find a correlate in the ANM mechanics of the mutants which corresponds to a measured loss of conductivity in experiments.

Additionally, we gain insight into the changes of the movements themselves, rather than the correlation among them as in the previous subsection. To this end, we decided to analyze the eigenvalues and respective eigenvectors for the wild type and mutant systems as well as for different mutants in more detail. Note, that the eigenvectors are restricted to entries, which are shared by the ΔN mutant pair under comparison. A comprehensive analysis of the $2 \times 3N$ eigenvectors constitutes a high-dimensional analysis problem, whose complexity needs to be reduced to make a comprehensive analysis possible.

We propose the following protocol: To compare a mutant or the wild-type (system I) to a mutant (system II), a distance matrix A is constructed computing the overlap distance of each eigenvectors u_I and u_{II} for all pairings (i,j) of eigenvectors (leaving out those belonging to the six vanishing singular values that occur due to rotational and translational degrees of freedom). This constitutes the overlap distance matrix A:

$$\mathbf{A}_{ij} = 1 - \frac{\mathbf{u}_{\mathrm{I},i} \cdot \mathbf{u}_{\mathrm{II},j}}{|\mathbf{u}_{\mathrm{I},i}||\mathbf{u}_{\mathrm{II},j}|} \tag{4}$$

By this definition, we provide for entries of A close to zero to indicate a high similarity of the respective eigenvector pairing (i,j). The matrix A is then used to assign corresponding eigenvectors/eigenmovements between the respective proteins. Although there are several efficient optimization schemes available [33–35], for practical purposes we restricted this step to a "greedy" approach of local optimization.

For these assignments, we computed histograms of the distribution of the similarity values contained in the A matrices. These histograms are then the sought-for, reduced representation of the similarity of the accessible space of eigenmovements of the various mutants in comparison to the functional wild-type structure or among each other.

As a potential falsification experiment, we repeated this for Δ1, Δ2, and Δ3 mutants. This allows the comparisons of the absolute changes in the various ΔN mutants, but also investigating the difference between two ΔN mutants, which differ by the same number of deleted residues. For example, we can test by this setup whether there is a fundamental distinction between the differences between the Δ1–Δ2 mutants in comparison to the differences between the Δ8–Δ9 mutants — therefore, accounting for any effect, which is caused by *relative* differences in the number of deleted residues. We can also check whether any significant change in the mechanics is due to the *absolute* number of deleted residues.

We continued and quantified the similarity between the histograms by computing the Kullback–Leibler divergences D_{kl} [36] between each histogram pair $h_{\Delta\Delta\mathrm{I}}$ and $h_{\Delta\Delta\mathrm{II}}$. D_{kl} was already discussed in the realm of molecular dynamics and chemoinformatics as a measure to quantify dynamical differences [37]:

$$D_{kl}(h_{\Delta\Delta\mathrm{I}} \| h_{\Delta\Delta\mathrm{J}}) = \sum_x h_{\Delta\Delta\mathrm{I}}(x) \log_2 \frac{h_{\Delta\Delta\mathrm{I}}(x)}{h_{\Delta\Delta\mathrm{II}}(x)} \tag{5}$$

In addition, we performed a clustering based on D_{kl} as distance measure [37].

All computations were performed using the package BioPhysConnectoR [38], an extension of the statistical software R [39] for biophysical and evolutionary biology purposes.

3. Results and discussion

In order to unravel the mechanical connectivity in the small K^+ channel Kcv we have chosen reduced molecular models to assess structural and functional modes in this protein. The rationale behind this approach is two-fold: a) the mathematical simplicity of such models allows investigating a large number of thought experiments and varying setups. This is orthogonal to a detailed account via, e.g., atomistic molecular dynamics simulations. Here, the loss of accuracy is compensated by a gain in overall insight on combinatorial many scenarios. Furthermore, b) we want to solely focus here on the dynamics of the protein around its native state. This avoids any complications with other selective pressures such as folding properties or more involved effects.

The full dynamical information, which can be derived from such reduced network models as the anisotropic network model (ANM), is contained within the mechanical covariance matrix (see Methods). The covariance matrix quantifies if and to what extent the fluctuations of the residues of a protein or a protein complex are 'related'. Each entry (i,j) of this matrix quantifies the in-phase or out-of-phase motion amplitudes of residues *i* and *j*. For every dynamic-causal relation between *i* and *j*, the respective entry in this matrix is large in absolute value. Furthermore, one obtains the (mechanical) correlation matrix from this covariance matrix by simple normalization. Since we are interested here in both the correlation and the amplitude of the motions themselves, we use both matrix types in our study. These matrices constitute the full mechano-dynamical information on a protein (complex) that can be extracted within the modeling accuracy of these ANMs. Typically, they compare well to more involved simulations as long as the protein dynamics resemble an equilibrium ensemble or at least has time-scales of conformational changes much longer than the time-scales to be investigated by the ANMs.

3.1. Truncation of the N-terminus

As a first domain of interest we concentrate on the N-terminal helix and its impact on the remaining part of the channel protein. An overview of the domains in the Kcv channel together with the amino acid sequence is shown in Fig. 1. It was previously shown that deletion of up to 7 N-terminal amino acids (L2-L8, referred to as Δ7 truncations) maintains activity of Kcv [15]. However, the channel becomes inactive if two more residues, T9 and R10, are removed as well; the intermediate Δ8 truncation (only T9 removed) shows only a reduced conductivity. The reason for the abrupt loss in channel function in response to the truncation of a single amino acid can be causally related to an interruption of the salt bridge pattern between the two TM domains [15]. To investigate whether the abrupt loss in function is also influenced by the dynamical modes of such ΔN-Terminus truncation, we developed a protocol for the truncated structures. The goal was to search for signals that go hand in hand with the complete loss of channel conductance when truncating 9 instead of 7 N-terminal residues, possibly only showing small signals for the Δ8 mutant. Since we did not incorporate any amino acid specificity in our model, we simply removed the first 7, 8 and 9 residues from the N-terminus, respectively. For completeness

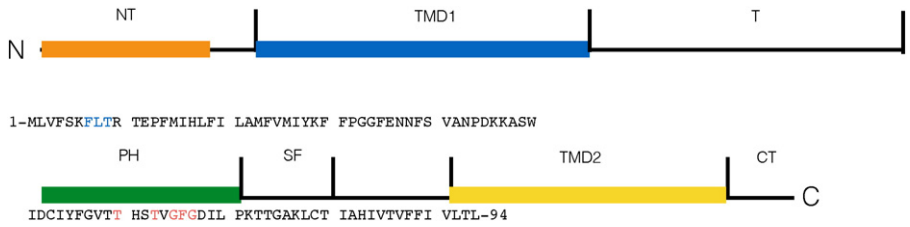

Fig. 1. Amino acid sequence of Kcv with assignment of functional domains. The functional domains above the sequence are taken from a homology model [21] and include the N-terminus (NT), transmembrane domains 1 (TMD1) and 2 (TMD2), the turret (T), the pore helix (PH), the selectivity filter (SF) and C-terminus (CT). The position of the N-terminal slide helix (SH, orange) the two transmembrane domains (blue, yellow) and the pore helix (green) are marked by bars. The canonical motive of K^+ channels is shown in red and the critical amino acids in the slide helix are highlighted in blue.

we removed in this analysis also the first amino acid methionine (M1). This is only possible in the theoretical protocol; in experimental studies M1 is essential for protein biosynthesis.

Since the covariance and correlation matrices of different ΔN-truncations have different lengths we restricted the analysis only to those entries of the covariance matrix, which correspond to the same residues in the different ΔN-truncations. To quantify which residues are most affected by shortening the N-terminus, we aggregated all squared differences belonging to each amino acid. The largest influence could be observed in the N- and C-terminal regions. This comes as no surprise, because both termini communicate mechanically with each other (see below). Interestingly, half of TMD1 was affected as well, whereas the remaining part showed only small deviations from the wild-type behavior (see Supplementary Fig. S1).

Furthermore, we also identified motions of the wild-type channel with those in the ΔN-truncations and compared them using the overlap distance (see Methods section for details on the procedure). By this procedure we obtained an aggregate picture of how the individual motions differ. We extended the set of mutants by Δ1, Δ2, and Δ3 mutants. This allows us to investigate whether substantial mechanical changes occur at an absolute number of truncated residues, or whether the effect is a relative one, e.g. would the truncation from Δ1 to Δ2 be as severe as the step from Δ8 to Δ9.

Previous studies [19,20,40] introduced the notion of functional and stabilizing mechanical motions, which can be classified by their respective frequencies. Modes with a low frequency represent global motions, which occur mainly due to functional movements e.g. conformational changes. High-frequency modes, on the other hand, are related to localized kinetics crucial for maintenance of structural stability. A pairwise comparison of the modes of both wild-type/mutant and mutant/mutant revealed high similarity mainly for stabilizing modes; the majority of the functional modes, however, differed substantially.

To analyze potential mechanical aberrations between different truncations we defined the intra-Δ and the inter-Δ group. The first group contains all comparisons between truncations, whose truncation lengths differ at most by two residues per monomer, e.g. truncations Δ1–Δ2 or Δ7–Δ9. The inter-Δ group is comprised of pairs in which the truncation lengths differ substantially such as Δ3–Δ8 or Δ1–Δ9.

Fig. 2 suggests two regimes for the truncation-truncation comparisons: the intra-Δ and inter-Δ group share common, distinct features among each other: mean, shape, location of the maximum in the histograms. The only deviation from this pattern is observed for the comparison of the Δ7–Δ9 truncations. In spite of belonging to the intra-Δ group, the Δ7–Δ9 overlap distances resemble the curvature of inter-Δ pairings. In other words, deleting two N-terminal residues from the Δ7-truncation introduced changes in the protein mechanics as drastic as

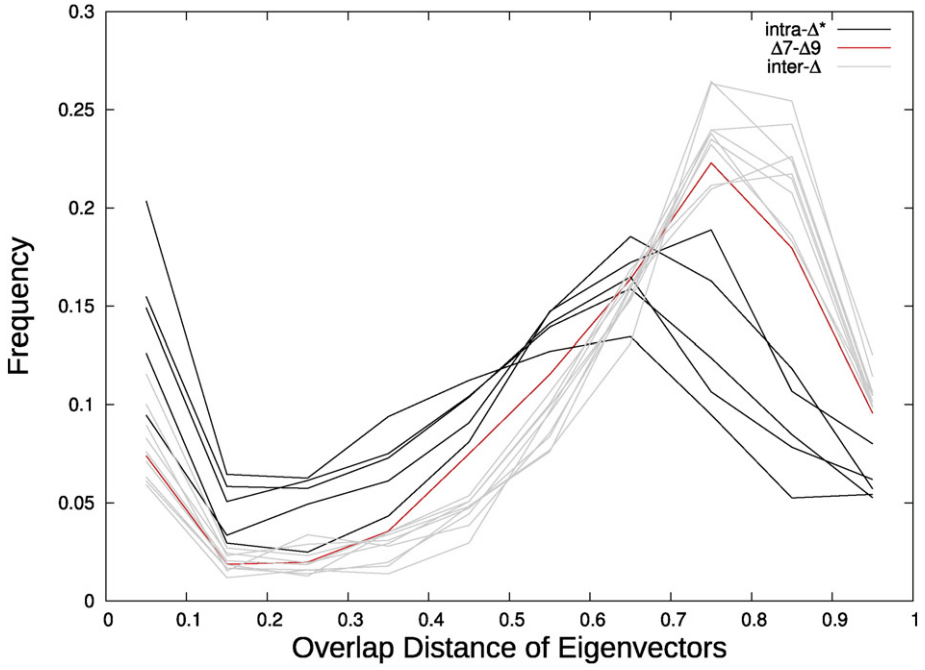

Fig. 2. Overlap distance histograms. Histograms of overlap distance values. For each Δ–Δ truncation pair the similarity is quantified as overlap distance of the eigenvectors/eigenmovements. Small overlap distances indicate a high similarity of the dynamics of the respective mutants. The intra-Δgroup includes mutants whose monomer sizes differ by one to three residues only (except Δ7–Δ9, highlighted in red) and the inter-Δ group comprises more pronounced truncation pairs, which differ in length by more than three residues. The distinct assignment of the red curve to the inter-Δ group is independent of the binning scheme.

deleting eight amino acids from the Δ1-mutant. This observation relates very well to the experimental results, which have shown that removing nine instead of seven residues of the N-terminus, rendered the channel inactive [15].

To quantify the effects shown in Fig. 2, we computed a distance measure between the respective histograms (the Kullback–Leibler divergence, see Supplementary information). The Kullback–Leibler divergence shows striking differences between the intra-Δ and the inter-Δ group (Fig. 3a). We found, that the truncation of the channel by a similar number of amino acids leads to similar changes in dynamics in general; this result is almost independent of the location of the truncation. The only exception from this rule is the comparison of the Δ7–Δ9 truncation. For this particular pair of truncation we see a remarkable difference: the changes induced by going from the Δ7 truncation to the Δ9 truncation is more severe than the modification of any other ΔL mutant to its respective $\Delta(L+1)$ or $\Delta(L+2)$ mutants; eventually the relative change is as severe as going for example from Δ1 to Δ8 mutant. This can also be seen in Fig. 3b, which presents the clustering of the mutant pairs in accordance with their Kullback–Leibler distances. Again, we observe that only the Δ7–Δ9 pair from the intra-Δ group is assigned to the inter-Δ group.

We further address the question whether the assignment of Δ7–Δ9 to the inter-Δ group rather than to the intra-Δ group results from specific, important interactions within the Kcv structure. Hence, we tested the sensitivity of our approach towards local changes. We identified the salt bridge, which is constituted of residues R10 and L94 in Kcv as a crucial interaction that is close to the truncation site [15]. To test whether this precise mutual interaction between the two amino acids is relevant for the mechanical coupling in the channel we repeated our protocol, but for all truncations this specific interaction was relaxed by a) pushing the residues farther apart or by b) weakening/deleting its interaction. Notably, with this procedure we obtained the same results as before. This implies that our protocol is insensitive towards local, small rearrangements and hence mutual interactions between amino acids; the results of these experiments underscore the exceptional character of the Δ7–Δ9 step, which is inherent in the global structure rather than in the local physicochemical interactions.

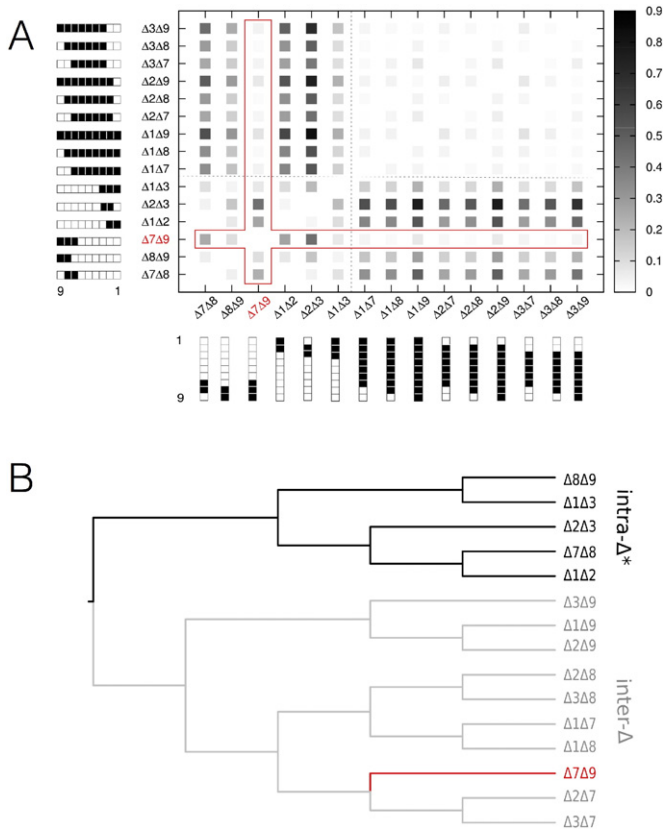

Fig. 3. Kullback–Leibler divergence of overlap distance histograms and resulting clustering. (A) Kullback–Leibler divergence of the overlap distance distributions. For each truncation pair, such as Δ7–Δ8 the overlap distance of the corresponding eigenvectors is computed as a measure for mechano-dynamical similarity. We compare those overlap distance distributions among all truncation-truncation pairs by the Kullback–Leibler divergence D_{kl} of the respective histograms; the shared deletions in each mutant-mutant pair are schematically illustrated next to the labels as white boxes. Small D_{kl} values (white to light-gray) indicate a high similarity of the underlying distributions. Note how the Δ7–Δ9 mutant (red) comparison is much closer to the group of mutants, which differ substantially, like Δ1-Δ7 or Δ3–Δ8, eventually showing signatures of the fundamental physiological changes found in vivo. (B) We computed a tree based on a clustering of the D_{kl} values. Clearly, the Δ7–Δ9 mutant pair is assigned to the inter-group. All results are insensitive to the binning scheme used for the frequencies in the D_{kl}.

Altogether, the analysis revealed that truncating more than 7 to 8 residues has a devastating effect on the dynamics of the channel. This altered dynamics in Kcv is correlated with the experimentally observed loss of channel activity; like in the computational analysis we found a sharp transition between active and inactive channels for a truncation of more than 7 to 8 amino acids [15]. The results further imply that the global protein structure is the main determinant of the dynamics in the pore module of this potassium channel. Clearly, the sequence has only an indirect effect as it needs to maintain the structure, thus the fold of the monomers and the assembled tetramer. A similar insensitivity of the molecular dynamics to (local) sequence variations – under fixed structure – was also found in other molecular complexes; the effect of the sequence on the dynamics is rather mediated via the protein fold [29].

The results of the analysis above strongly support the finding that the N-terminus serves as a transmitter of conformational changes from upstream elements to gating in the channel pore module. This conclusion is further supported by experimental data, which show that the critical region between amino acid 7 and 9 in the N-terminus of Kcv is also relevant in the synthetic voltage sensitive Kvc_{synt} for the functional coupling between the voltage sensor and the channel gate [18]. The overall good agreement between the independent computational predictions and experimental data support the view that ANMs are a suitable tool for uncovering structure/function correlates in the small K^+ channel.

3.2. Single switch-off of interactions to investigate importance of individual interactions

To gain further insight into the tectonics, e.g. on the functional connectivity between the N-terminus of Kcv and other functional domains of the channel, we applied a protocol in which single non-covalent contacts were artificially deleted in all monomers simultaneously, in analogy to an established protocol [19]; all other interactions of the corresponding residues were left untouched. Connections between subunits were retained and the effect was quantified by the Frobenius norm of the covariance matrices. This protocol was already successfully applied previously to the HIV1 protease to identify important contacts (in contrast to whole residues) for the biomechanics of this protein [19].

With the specific interest on the role of the N-terminus on channel gating, we illustrate in Fig. 4 the results of single switch offs on the C-terminus. This is valid considering that the negatively charged C-terminus functions as a gate in the Kcv channel [14,15]. For each existing contact, excluding those with at least one residue belonging to the C-terminal region, the Frobenius norm is shown.

Above all, the data show that deleting interactions of amino acid M1 with other amino acids in the N-terminus leads to major changes in the mechanics of the C-terminus. Worth noting is that the importance of this amino acid can only be appreciated in computational studies since this amino acid cannot be replaced in experiments. In addition to contacts in the N-terminus the analysis also reveals large effects of contacts between both transmembrane domains TMD1 and TMD2 on the C-

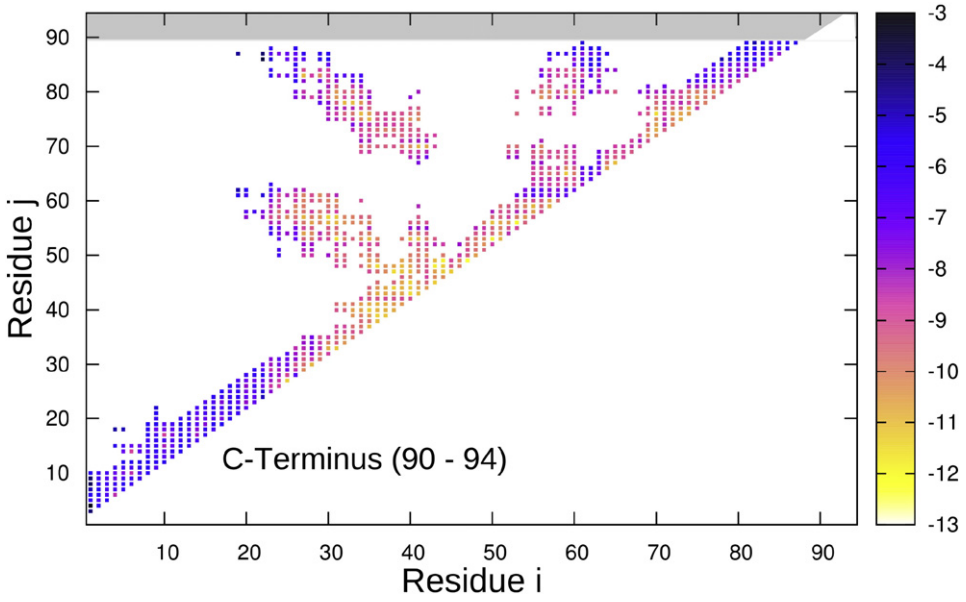

Fig. 4. Frobenius Norm for C-terminal residues in single-switch-off. Single switch-off results for the C-terminus. Each interaction of contacting residues (i,j) that are not classified as C-terminal residues (indicated by the shaded area) is switched off one at a time in all chains simultaneously. The Frobenius norm is computed for C-terminal parts of the covariance matrices. Blue colors indicate interactions having a high influence on the dynamics of the C-terminus, whereas yellow interactions are negligible.

terminus. The most significant residue contacts are between the pairs: F19-V87, A22-T86 and A22-V87 (see Table 1). Important to note here are two things: the analysis again highlights the region around amino acid 20 in TM1, which was already in previous experimental studies identified as a key amino acid for gating and for long range interactions in the Kcv channel. Mutations of AA 19 and 20 for example are able to alter the gating properties and the susceptibility of block by Ba^{2+} in the Kcv channel [41,42]. The analysis also underscores an interaction of TMD1 with the mobile part of TMD2 e.g. amino acids downstream of His82 [23]. From MD simulations it is known that the mobility of the lower part of TMD2 is important for the channel gate at the entry to the cavity [14,21]. Altogether the data confirm a functional significance of contacts within the N- and between the TMDs with an impact on the mechanics of the C-terminus. Therefore, motions in the N-terminus as well as connections between the TMD can be transmitted to a potential gate of the Kcv channel.

The same analysis was performed for all other functional domains namely the N-terminus, TMD1, TMD2, the turret, the pore and the filter region. Table 1 and Fig. 5 shows the top 5 contacts ranked according to their influence on the respective regions measured on the basis of their Frobenius norms. The results again highlight the functional significance in TMD1 around amino acid 20 and even more so the role of the N-terminus on the overall mechanics of Kcv. While this domain contributes only 13% of the entire protein, 40% of the top-scored interactions include an amino acid from the N-terminus in the pairwise interaction (Table 1). More than half of these interaction partners in the N-terminus are located on the portion of the N-terminus, which was found crucial in the analysis of Fig. 3 and in experiments in which the N-terminus was sequentially truncated [15]. The data suggest that the N-terminus and in particular the amino acids downstream of amino acid L8 form multiple contacts with different amino acids in their

Table 1
Contacts with major influence on the dynamics of specified channel regions. Results for single switch-off experiments. For each region (as defined in Figs. 1 and 5) the contacts with the highest influence (quantified by the Frobenius norm of respective covariance matrix portions) on the dynamics of the respective region are listed. Contacts, which include an amino acid from the N-terminus are highlighted in yellow.

SH	TMD1	T	PH	SF	TMD2	C
E12-L94	E12-L94	D52-D68	A22-L94	F19-S62	E12-L94	M1-F4
T11-L94	L92-L94	D68-K72	T9-A22	F19-H61	A22-L94	A22-T86
L18-L94	T9-T93	F24-I51	E12-L94	M1-I90	S5-I90	M1-L8
A22-L94	T11-L94	D68-P71	L18-F24	I69-I81	T11-L94	M1-T9
L18-T20	S5-L92	P32-D52	M1-I90	M1-V91	T9-A22	A22-V87

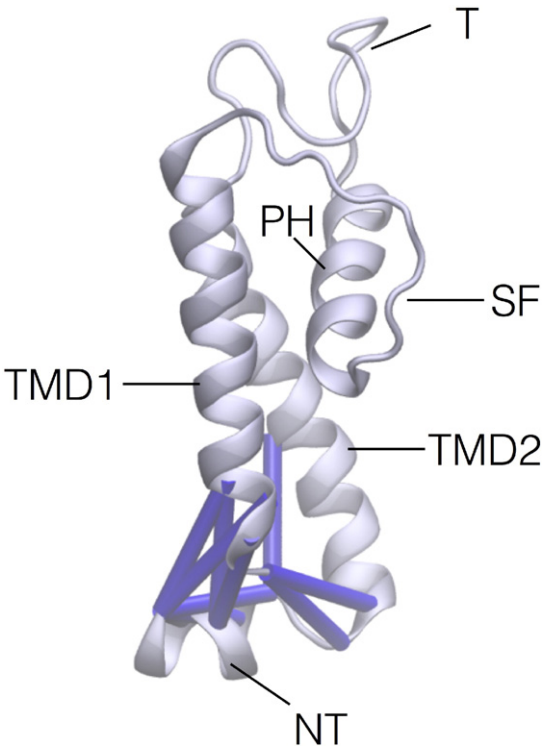

Fig. 5. Mechanical coupling of N-terminus with other domains in Kcv channel. Monomer of Kcv channel with cytoplasmic N-terminus (NT), the outer (TMD1), the inner transmembrane domain (TMD2), the pore helix (PH), the turret (T) and the selectivity filter motive (SF). The 8 main contacts from Table 1, which involve an amino acid in the N-terminus, and which cause significant change of displacement when switched off are indicated by cylinders.

vicinity and that these interactions have a major impact on the mechanics of all functional domains in the channel; only the turret seems to be unaffected by the N-terminus. A graphical presentation of the top scoring interactions of N-terminal amino acids with amino acids outside the N-terminus is shown in Fig. 5. The data illustrate that the majority of the functionally important interaction are between different parts of the N-terminus and the last 4 amino acids in the C-terminus. The most prominent contact, which affects the mechanics of nearly every functional domain, is that between E12 and the C-terminal AA L94.

4. Conclusion

Reduced molecular models are capable to generate a global map for the mechanical connections in a small K^+ channel. This map provides detailed information on long-distance interactions in this miniature channel, which cannot be directly explained by mutual interactions of amino acids. The good agreement between the simulation data and experimental results furthermore implies that ANM models are suitable for understanding the dynamics of K^+-channel proteins. As a quality control we find that some of the main mechanical interactions in the Kcv channel, which were identified from the network model, are in agreement with experimental results, which have suggested long-range interactions between the outer TMD domain and the pore in this channel [22,41,42]. Beyond this, the ANM also shows that a truncation of the N-terminus of Kcv beyond a critical length has a devastating effect on the channel structure and that this truncation is correlated with a loss of experimentally detectable channel function [15]. The data furthermore highlight that parts of the N-terminus form multiple interactions with neighboring domains with a profound impact on the mechanics of key domains in the channel. The latter also includes domains like the filter, the pore and the C-terminus e.g. domains, which were already identified as potential gates in the Kcv channel [13–15]. Taken together, the data support the view, that movements of the N-terminus can indeed be transmitted via long-range interactions to the gates of the channel.

In the particular case of the N-terminus, our results demonstrate that important mechanical properties are governed predominantly by the protein topology. These functional modes presumably determine generic mechanical interactions in a K^+ channel. Any precise and channel specific feature, which is characteristic for a certain type of K^+ channel with the same pore architecture, is then modulated on top of these genuine modes by specific amino acid interactions.

Interestingly, we found that the topology of the channel complex alone is responsible for all of the generic effects summarized above. This suggests, that the molecular evolution has folded the monomers and shaped the tetramer structure to a topology solely responsible for the dynamical effects necessary to explain the experimental findings discussed above. Therefore, sequence details seem to have only an implicit effect on the coarse-grained dynamics via the fold and not through biochemical details at a smaller scale. This finding suggests, that the dynamical effects are merely caused by the structure alone; they can only slightly be altered by local changes. The same effect was already found for the bacterial ribosome [31]. We believe, that this observation has interesting implications for the rational design of functional channels. We hypothesize that one needs – at least for the coarse-grained scale – only a structural model and not a particular sequence to assess the molecular dynamics and not concern oneself with the particulars of the (local) biochemistry. Note, that this applies only to the dynamics of the protein, and not to the physical chemistry of, e.g., the ion transport process.

Conflict of interest

We declare that we have no conflict of interests.

Acknowledgments

We are grateful to Prof. Dan Minor (USSF) for helpful suggestions to the manuscript and we acknowledge financial support from the Deutsche Forschungsgemeinschaft (grants HA 5261/3-1, TH 558/29-1) and from the Landes-Offensive zur Entwicklung Wissenschaftlich-ökonomischer Exzellenz (LOEWE) initiative iNAPO to K.H. and G.T.

Appendix A. Supplementary data

Supplementary data to this article can be found online at http://dx.doi.org/10.1016/j.bbamem.2015.09.015.

References

[1] C. Miller, An overview of the potassium channel family, Genome Biol. 4 (2000) 1–5.
[2] D.A. Doyle, J.M. Cabral, R.A. Pfützner, A. Kuo, J.M. Gulbis, S.L. Cohen, B.T. Chait, R. MacKinnon, The structure of the potassium channel: molecular basis of K^+ conduction and selectivity, Science 280 (1998) 69–76.
[3] B. Hille, Ion Channels of Excitable Membranes, third ed. Sinauer Associates, Inc., Sunderland, Massachusetts, USA, 2001.
[4] R. MacKinnon, Potassium channels, FEBS Lett. 555 (2003) 62–65.
[5] M. Lolicato M, et al, Cyclic dinucleotides bind the C-linker of HCN_4 to control channel cAMP responsiveness. Nat. Chem. Biol. 10 (2014) 457–462.
[6] F.M. Ashcroft, F.M. Gribble, Correlating structure and function in ATP-sensitive K^+ channels, Trends Neurosci. 21 (1998) 288–294.
[7] K.B. Craven, W.N. Zagotta, CNG and HCN channels: two peas, one pod, Annu. Rev. Physiol. 68 (2006) 375–401.
[8] Q. Li, et al., Structural mechanism of voltage-dependent gating in an isolated voltage-sensing domain, Nat. Struct. Mol. Biol. 21 (2014) 244–252.
[9] F. Bezanilla, How membrane proteins sense voltage, Nat. Rev. Mol. Cell Biol. 9 (2008) 323–332.
[10] G. Thiel, D. Baumeister, I. Schroeder, S.M. Kast, J.L. Van Etten, A. Moroni, Minimal art: or why small viral K^+ channels are good tools for understanding basic structure and function relations, Biochim. Biophys. Acta 1808 (2011) 580–588.
[11] S. Gazzarrini, M. Severino, M. Lombardi, M. Morandi, D. DiFrancesco, J.L. VanEtten, G. Thiel, A. Moroni, The viral potassium channel Kcv: structural and functional features, FEBS Lett. 552 (2003) 12–16.
[12] F.C. Chatelain, S. Gazzarrini, Y. Fujiwara, C. Arrigoni, C. Domigan, G. Ferrara, C. Pantoja, G. Thiel, A. Moroni, D.L. Minor, Selection of inhibitor-resistant viral potassium channels identifies a selectivity filter site that affects barium and amantadine block, PLoS One 4 (2009), e7496.
[13] A. Abenavoli, M. DiFrancesco, I. Schroeder, S. Epimashko, S. Gazzarrini, U.P. Hansen, G. Thiel, A. Moroni, Fast and slow gating are inherent properties of the K^+ channel pore module, J. Gen. Physiol. 134 (2009) 869–877.
[14] S. Tayefeh, T. Kloss, G. Thiel, B. Hertel, A. Moroni, S. Kast, Molecular dynamics simulation of the cytosolic mouth in Kcv-type potassium channels, Biochemistry 46 (2007) 4826–4839.
[15] B. Hertel, S. Tayefeh, T. Kloss, J. Hewing, M. Gebhardt, D. Baumeister, A. Moroni, G. Thiel, S.M. Kast, Salt bridges in the miniature viral channel Kcv are important for function, Eur. Biophys. J. 39 (2010) 1057–1068.
[16] C. Arrigoni, I. Schroeder, G. Romani, J.L. Van Etten, G. Thiel, A. Moroni, The voltage-sensing domain of a phosphatase gates the pore of a potassium channel, J. Gen. Physiol. 141 (2013) 389–3895.
[17] C. Cosentino, et al., Engineering of a light-gated potassium channel, Science 348 (2015) 707–710.
[18] M.L. DiFrancesco, S. Gazzarrini, C. Arrigoni, G. Romani, G. Thiel, A. Moroni, Engineering a Ca^{2+} sensitive (bio) sensor from the pore-moduke of a potassium channel, Sensors 15 (2015) 4913–4924.
[19] K. Hamacher, Relating sequence evolution of HIV1-protease to its underlying molecular mechanics, Gene 422 (2008) 30–36.
[20] I. Bahar, A.R. Atilgan, M.C. Demirel, B. Erman, Vibrational dynamics of folded proteins: significance of slow and fast motion in relation to function and stability, Phys. Rev. Lett. 80 (1998) 2733–2736.
[21] S. Tayefeh, et al., Model development for the viral Kcv potassium channel, Biophys. J. 96 (2009) 485–498.
[22] M. Gebhardt, L. Henkes, S. Tayefeh, B. Hertel, T. Greiner, J. Van Etten, D. Baumeister, C. Cosentino, A. Moroni, S.M. Kast, G. Thiel, The Relevance of Lysine Snorkeling in the Outer Transmembrane Domain of Small Viral Potassium Ion Channels, Biochem. 51 (2012) 5571–5579.
[23] M. Gebhardt, F. Hoffgaard, K. Hamacher, S.M. Kast, A. Moroni, G. Thiel, Membrane anchoring and interaction between transmembrane domains is crucial for K^+ channel function, J. Biol. Chem. 286 (2011) 11299–11306.
[24] I. Bahar, A.R. Atilgan, B. Erman, Direct evaluation of thermal fluctuations in proteins using a single-parameter harmonic potential, Fold. Des. 2 (1997) 173–181.
[25] A. Atilgan, S.R. Durell, R.L. Jernigan, M.C. Demirel, O. Keskin, I. Bahar, Anisotropy of fluctuation dynamics of proteins with an elastic network model, Biophys. J. 80 (2001) 505–515.
[26] C. Micheletti, P. Carloni, A. Maritan, Accurate and efficient description of protein vibrational dynamics: comparing molecular dynamics and Gaussian models, Proteins 55 (2004) 635–645.

[27] P. Doruker, R.L. Jernigan, I. Bahar, Dynamics of large proteins through hierarchical levels of coarse-grained structures, J. Comput. Chem. 23 (2002) 119–127.
[28] L. Yang, G. Song, A. Carriquiry, R.L. Jernigan, Close correspondence between motions from principal component analysis of multiple HIV-1 protease structures and elastic network modes, Structure 16 (2008) 321–330.
[29] K. Hamacher, J.A. McCammon, Computing the amino acid specificity of fluctuations in biomolecular systems, J. Chem. Theory Comput. 2 (2006) 873.
[30] M.M. Tirion, Large amplitude elastic motions in proteins from a single-parameter Atomic Analysis, Phys. Rev. Lett. 77 (1996) 1905–1908.
[31] K. Hamacher, K. Trylska, J.A. McCammon, Dependency map of proteins in the small ribosomal subunit, PLoS Comput. Biol. 2 (2006), e10.
[32] W.H. Press, S.A. Teukolsky, W.T. Vetterling, B.P. Flannery, Numerical Recipes in C, Cambridge University Press, 1995.
[33] K. Hamacher, Adaptation in stochastic tunneling global optimization of complex potential energy landscapes, Europhys. Lett. 74 (2006) 944–950.
[34] K. Hamacher, Adaptive extremal optimization by detrended fluctuation analysis, J. Comput. Phys. 227 (2007) 1500–1509.
[35] K. Hamacher, Energy landscape paving as a perfect optimization approach under detrended fluctuation analysis, Phys. A 378 (2007) 307–314.
[36] S. Kullback, R.A. Leibler, On information and sufficiency, Ann. Math. Stat. 22 (1951) 79–86.
[37] K. Hamacher, Information theoretical measures to analyze trajectories in rational molecular design, J. Comput. Chem. 28 (2007) 2576–2580.
[38] F. Hoffgaard, P. Weil, K. Hamacher, BioPhysConnectoR: connecting sequence information and biophysical models, BMC Bioinf. 11 (2010) 199.
[39] Development Core Team R, A Language and Environment for Statistical Computing. Manual, 2008.
[40] K. Hamacher, Temperature dependence of fluctuations in HIV1-protease, Eur. Biophys. J. 39 (2010) 1051–1056.
[41] M. Kang, A. Moroni, S. Gazzarrini, D. DiFrancesco, G. Thiel, M. Severino, J.L. Van Etten, Small potassium ion channel protein encoded by chlorella viruses, Proc. Natl. Acad. Sci. U. S. A. 101 (2004) 5318–5324.
[42] S. Gazzarrini, M. Kang, J.L. Van Etten, S. Tayefeh, S.M. Kast, D. DiFrancesco, G. Thiel, A. Moroni, Long-distance interactions within the potassium channel pore are revealed by molecular diversity of viral proteins, J. Biol. Chem. 279 (2004) 28443–28449.